Aerosol Route to Highly Efficient (Co)Mo/SiO_2 Mesoporous Catalysts

*Frédéric Colbeau-Justin, Cedric Boissière, Alexandra Chaumonnot, Audrey Bonduelle, and Clément Sanchez**

One-pot aerosol-assisted synthesis of mesostructured (Co)Mo/SiO_2 catalysts with high hydrogenation activity is reported. The evaporation*induced self-assembly mechanism of the formation of such catalysts enables optimized interactions between each component, resulting in the tuning of localization of the active species. The high activity is probably associated with the original morphology of the active phase as well as the creation of relevant defects in its structure. Since spray-dried mesoporous CoMo/SiO_2 catalysts outperform the hydrogenation activity of classical impregnated catalysts, aerosol route appears to be a promising way for the industrial-scale preparation of new highly efficient hydrocarbons catalysts.

1. Introduction

The global fuel market demand strives for more environmental-friendly product. As a consequence, fuel specifications are being ever more stringent. On the other hand, the price of light crude oil is continuously increasing. In this context, the challenging development of cheap and very active heterogeneous catalysts is of particular interest for the refiners. Among the different catalytic processes that take place in petroleum refining, hydrotreatment (HDT) is a key process since it enables the abatement of heteroatom, responsible for environmental issues and facilities damages. For industrial purposes, conventional hydrotreating catalysts are usually obtained by incipient wetness impregnation on ceramic oxide of the oxometallic elements (Co,Mo), which are the precursors of the promoted active phase (Co-MoS_2). The latter is obtained via subsequent sulfidation treatment. This synthetic pathway suffers different drawbacks such as the large number of preparation steps and the perfectible dispersion of the active phase on the oxide surface. As a consequence, the amount of oxo-species must be optimized to avoid crystallization of bulk $CoMoO_4$ or MoO_3, which are refractory to the sulfidation.[1] So far, no direct method exist for preparing at the same time both a mesoporous ceramic matrix and the active phase ideally dispersed. A better dispersion of oxometallic phase on ceramic support may be obtained by the mean of sol-gel procedures[2,3] as well as the use of additives such as phosphorus.[4,5] In this particular case, the precursor of the oxometallic phase is often a phosphomolybdic heteropolyacid (HPA). The sol-gel process most often relies on the consecutive hydrolysis and condensation of metal alkoxide precursors which can be advantageously coupled with the use of amphiphilic molecules for inducing a mesostructured porosity.[6–8] The electrostatic interaction between sol-gel oligomers, surfactant and HPA species enables the formation of composite materials where the latter are trapped in a ceramic matrix.[9,10] Although this method allows a good dispersion of oxo-species within the composite, their localization in the wall of the support may hinder their accessibility and then decrease the activity of the catalyst. As a matter of fact, the interaction between HPA and micelles drives the localization of the oxo-metallic species in the material. So far, such synthetic approach does not allow to incorporate at the same time HPA precursors and a metal promotor (Co(II) or Ni(II) centres).

In the present work we report the first synthetic protocol allowing the direct synthesis of mesoporous silica already loaded with cobalt and molybdenum precursors needed for the preparation of Co:MoS_2 catalysts. By using an original and low cost aerosol method, we successfully produced some mesoporous CoMo/SiO_2 composites with a very good active_phase_localization/catalytic_activity compromise. This process has recently emerged as very efficient for insuring a perfect control of catalytic centres,[11] stoichiometry and dispersion, while allowing at the same time the creation of mesoporosity via Evaporation Induced Self Assembly of amphiphilic templates.[12,13] By promoting the co-location of molybdenum HeteroPolyAnion (HPA) precursor nearby micelles of non-ionic structuring agent during the evaporation of aerosol droplets, we insured in one step a complete accessibility of the active phase of the mesostructured catalyst for sulfidation of molybdenum canters. This co-location could be obtained by adjusting the interaction between HPA and surfactant as well as the kinetics of hydrolysis-condensation of the silica matrix precursors. The spraying of the solution of precursors, allowed the formation of individual droplets containing homogeneous content of

Dr. F. Colbeau-Justin, Dr. C. Boissière,
Prof. C. Sanchez
Laboratoire Chimie de la Matière Condensée
UMR UPMC-Collège de France
11 place Marcelin Berthelot, 75231, Paris, France
E-mail: clement.sanchez@upmc.fr
A. Chaumonnot, A. Bonduelle
IFP Energies Nouvelles – Etablissement de Lyon
Rond-point de l'échangeur de Solaize
BP 3, 69360, Solaize, France

DOI: 10.1002/adfm.201302156

precursors. The resulting catalysts obtained by fast drying of these droplets are spherical particles which retain perfectly the stoichiometry of the pristine solution with a very good dispersion of all precursors. A catalytic test (hydrogenation of toluene) was used to investigate the catalytic properties of cobalt promoted MoS_2 active phase obtained by this process in order to determine the potential interest of such a synthetic approach for the synthesis of hydrotreating catalysts.

2. Results and Discussion

2.1. Synthesis and Characterization of Oxidic Mesoporous (Co)Mo/SiO_2 Composites

In a typical synthesis, an aqueous solution of hydrolyzed tetraethyl orthosilicate (TEOS) is blend with a solution of HPA ($H_3PMo_{12}O_{40}$, 10 wt% of MoO_3 in the calcined material) with or without $Co(OH)_2$ (Co/Mo = 0.36 mol) and a solution of block-copolymer Pluronic P123 $[EO]_{20}$-$[PO]_{70}$-$[EO]_{20}$. The resulting solution is sprayed with a Büchi B-290 spray drier. The hybrid material is then calcined under static air (350 °C for 12 h) to remove the surfactant. Catalysts with 20% wt. of MoO_3 in the calcined material were also prepared by the same method. As a reference, a pure mesoporous silica was prepared by the same aerosol method, using the same precursor solution but without any cobalt nor HPA. This mesoporous silica, labelled *SiO_2Aero* has been loaded by wetness impregnation of an aqueous solution of $Co(OH)_2$ and HPA precursors (Co/Mo molar ratio similar to that used for the direct synthesis of the catalyst) for creating reference catalysts with similar porous mesostructure (pore size, tortuosity, porous volume and particle morphology) and heat treated at the same temperature of 350 °C for 12 h. These latter materials are labeled *SiMoX* and *SiCoMoX* where X stands for the synthesis procedure: *Aero* for the direct aerosol-assisted synthesis of the catalyst containing Co and HPA, and *Imp* for post-impregnated active phase into the pure mesoporous silica reference. Such impregnated samples were prepared in order to compare the efficiency of the dispersion of the metallic precursors by both methods.

All aerosol mesoporous materials (Co)Mo/SiO_2 catalysts and the pure mesoporous silica sample have a spherical shape with a diameter ranging between 100 nm and 20 µm. Particles with a diameter below 1 µm are solid. For larger diameter, particles are hollow (**Figure 1**A). We analysed that about 90 wt% of the catalyst is made of hollow particles. This morphology is intrinsic to the Buchi B290 spray dryer device, used with a fixed molar ratio ethanol/water of 0.06. Both solid and hollow particles show a regularly organized mesoporosity, evidenced by TEM (Figure 1B). Mesostructuration of each material is confirmed by small angle X-ray scattering. The measured d-spacing value is almost equivalent (~10.5 nm) for *SiMoAero* and *SiCoMoAero* materials than for pure SiO_2 (Figure 1C). Then, it is interesting to point out that the simultaneous presence of oxospecies of Mo and Co does not trouble the mesostructuration. Nitrogen physisorption isotherm (Figure 1D) of each material shows a capillary condensation with hysteresis cycle stemming from mesostructured material exhibiting periodically ordered pores of about 8 nm (see SI-1 for BJH plots). Subtracting the average pore size from the d-spacing allows estimating a wall thickness of about 2.5 nm for *SiCoMoAero* and *SiO_2Aero* materials whereas the calculated wall thickness of *SiMoAero* material is about 3.2 nm. This can indicate that the localization of the oxometallic phase may be different according to the presence or the absence of cobalt. Larger wall thickness may be reached when Mo is located inside the silica wall. The fact that SiCoMoAero material shows the same wall thickness than pure silica can be due to the localization of the oxometallic phase outside of the silica matrix, that is, either inside the organic domain and/or outside particles. The other textural and structural parameters

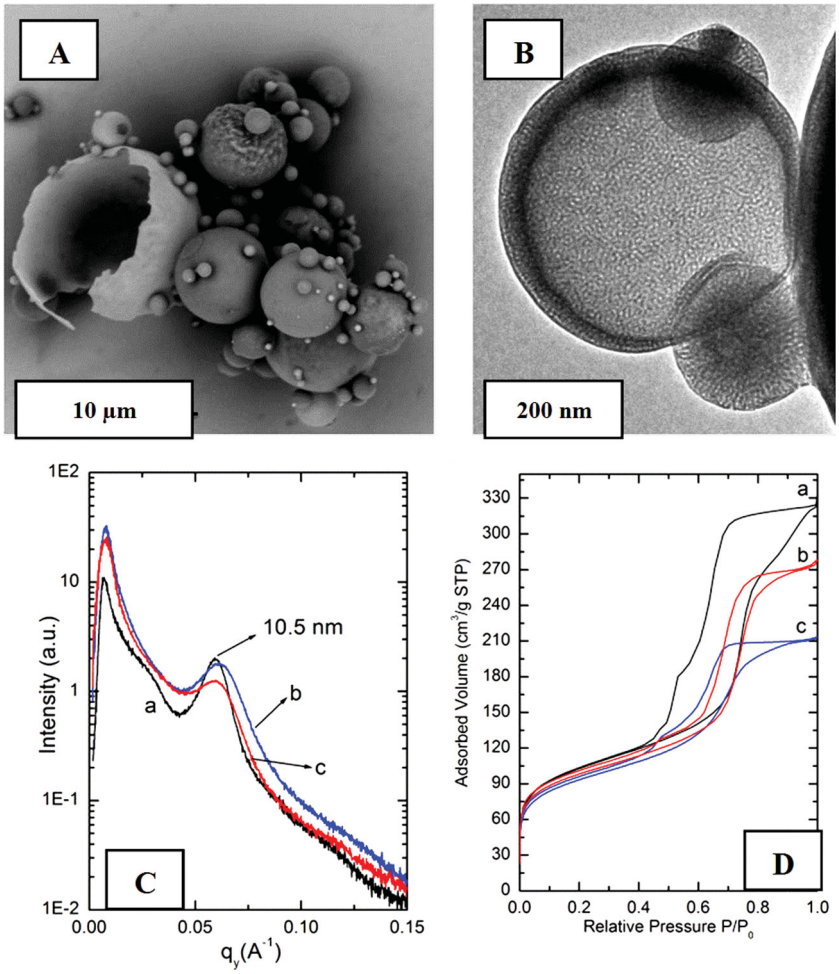

Figure 1. A,B) SEM and TEM pictures of calcined SiCoMoAero; C) SAXS plot for calcined a) SiO_2Aero b) SiMoAero and c) SiCoMoAero; D) N_2 adsorption-desorption isotherms of a) SiO_2Aero b) SiMoAero and c) SiCoMoAero.

Table 1. Textural and structural properties of the spray-dried materials.

Materials	BET SSA [m^2/g]	Pore width [nm][a)]	Pore volume [cm^3/g][b)]	Micropore volume [cm^3/g][b)]	d-Spacing [nm][c)]	Wall thickness [nm][d)]
SiO_2Aero	296	8.2	0.45	0.00	10.6	2.4
SiMoAero 10%	260	7.0	0.32	0.04	10.2	3.2
SiMoAero 20%	62	6.9	0.07	0.01	10.2	3.3
SiCoMoAero 10%	278	8.0	0.42	0.05	10.5	2.5
SiCoMoAero 20%	236	8.9	0.40	0.04	10.7	1.8

Obtained from: [a)]BJH method; [b)]t-plot method; [c)]Small angle X-rays scattering (SAXS) measurement; [d)]the relation wall thickness = d-spacing – pore width.

are summarized in **Table 1**. We highlight here that no CoO nor MoO_3 could be observed by high-resolution transmission electron microscopy (HR-TEM) or X-ray diffraction (XRD) after thermal treatment à 350 °C which points out a homogeneous dispersion of metallic precursors within the mesoporous materials directly prepared by aerosol. Scanning electron microscopy coupled with energy-dispersive X-ray spectroscopy (SEM-EDX) cartographies of molybdenum (**Figure 2**A and B) and cobalt (Figure 2C and B) of post-impregnated silica clearly show spots of higher concentration, characteristic of poor dispersion. Conversely, the cartography of the one-pot aerosol synthesized SiCoMoAero material, confirms that the dispersion obtained by spray-drying is homogeneous. Furthermore, the XRD pattern of SiCoMoAero shows no peaks whereas that of SiCoMoImp shows small crystallites of hydrated $H_3PMoO_{12}O_{40}$ (**Figure 3**). The same trends can be observed with SiMoAero compared with SiMoImp material.

2.2. Characterization of Sulfided Mesoporous Co-MoS_2/SiO_2 Composites

Spray-dried and impregnated materials have been sulfided under H_2S/H_2 atmosphere during 2 h at 350 °C. Sulfided materials were characterized by X-ray photoelectron spectroscopy (XPS) and TEM. A systematic decomposition of the XPS Mo(3d) and Co(2p) peaks has been performed in order to estimate the MoS_2 and Co-MoS_2 quantities (**Table 2**). The poor dispersion of Mo and Co for the impregnated samples leads to the formation of a large amount of Co_9S_8 to the detriment of the catalytic active phase Co-MoS_2. This result is certainly due to the heterogeneity of the molar ratio Co/Mo[14] which can be locally higher than the average of 0.36. Concerning aerosol synthesized materials, the results are close to that of the industrial reference, which is an alumina impregnated with Co and Mo (optimized Co/Mo molar ratio).

The presence of MoS_2 slabs is clearly visible on TEM images (**Figure 4**). Impregnated catalysts exhibit long MoS_2 slabs (>10 nm average), while aerosol made material exhibit much shorter slabs (about 5 nm), closer from the average slab length of the industrial reference (3.5 nm). It can be observed on SiCoMoAero pictures numerous cross MoS_2 slabs which look curved and/or entangled. A similar behavior is also observed with impregnated catalysts. Such effects (absent in the industrial catalyst which exhibits much shorter slabs) can be due to the growth of these slabs in a confined space such as a mesopore of the matrix. This unusual behavior is combined with high cobalt promotion efficiency only when cobalt and molybdenum precursors are both present in the initial sol. This high promotion rate can only be explained by easy access and close localization of cobalt and HPA precursors during sulfidation reaction. During the materials processing, this means that a cobalt-driven modification of two main physico-chemical effects happens: i) an optimized attractive interaction between Co, Mo precursors and the surfactant. Indeed, Co^{2+} can be strongly complexed by the polyethylene oxide chains of the surfactant. As the molybdenic precursor is a polyanion, it will be drained by the Co^{2+} inside the micelle for respecting electroneutrality during the evaporation of each droplet of solution as schemed in **Figure 5**. ii) With the introduction of the cobalt hydroxide precursor, the pH of the sol is 4.5 and silica oligomers have a net neutral to slightly negative charge which exhibit poor attractiveness for polymolybdate anions if compared with complexed Co^{2+} sites. By contrast, when the

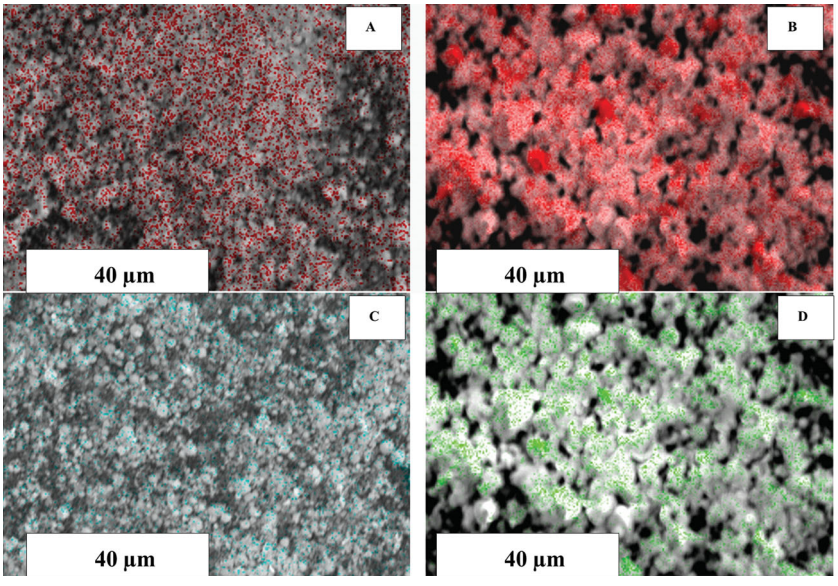

Figure 2. SEM-EDX molybdenum cartography of A) SiCoMoAero and B) SiCoMoImp SEM-EDX cobalt cartography of C) SiCoMoAero and D) SiCoMoImp.

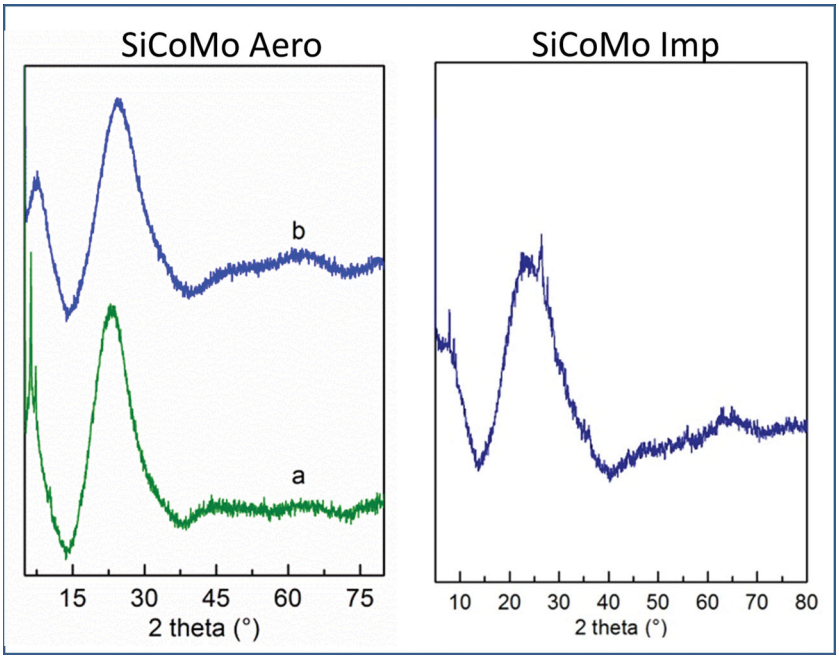

Figure 3. XRD pattern of A) a) as-made and b) calcined SiCoMoAero 20% and B) SiCoMoImp 20%.

cobalt precursor is not introduced, the pH of the sol remains at 2. Hydrated PEO coronas of micelles have then no intrinsic affinity for polyanions due to the negative partial charge of PEO oxygens.[15] At this pH, slightly positive or neutral silica oligomers are prone to electrostatically interact with the negative polyanions. As EISA goes on, polymolybdate species are mainly trapped inside the silica walls resulting to the enlargement of the silica wall thickness of the mesoporous catalyst.

As a consequence, the spray drying process has the very favorable effect to produce particles with homogeneous repartition of metal centres, as well as to allow the co-location of both molybdenum precursor and cobalt promotor at the surfactant/silica interface of each particle. In Table 2, the difference of MoS_2 slab length and promotion efficiency observed between the impregnated and the spray dried materials is then very probably due to the quality of the dispersion of the oxometallic phase, the poor quality of dispersion of the impregnated material leading to domains with longer MoS_2 slabs and domains without MoS_2 slabs at all. Concerning the SiMoAero materials, it is interesting to point out that MoS_2 slabs are smaller than SiCoMoAero ones and they are not appearing as entangled. The localization of the molybdenum inside the wall can explain these observations as the diffusion of the H_2S is much more limited in a wall than at the surface of a mesopore.

2.3. Catalytic Hydrogenation of MoS_2/SiO_2 and Co-MoS_2/SiO_2 Composites

The catalysts were tested in the model reaction of hydrogenation of toluene for determining if the active phase obtained from aerosol made materials was suitable for catalysis application.

2.3.1. Non-promoted Catalysts

As expected, specific activities of the non-promoted catalyst is much lower than that of promoted catalysts, as shown in **Table 3**. Furthermore, the spray-dried *SiMoAero* sample shows a hydrogenation activity slightly lower than that of its impregnated counterpart (not shown here). This effect is likely to be due to the absence of cobalt during the drying of *SiMoAero* material that promotes HPA trapping within the silica walls. The result of this is an active sulfided phase probably partially trapped within the silica walls (Figure 4C), thus with a limited number of accessible catalytic sites.

2.3.2. Promoted Catalysts

For cobalt-promoted catalysts, hydrogenation specific activities of impregnated samples, that is the relative activity per MoS_2, are lower than those of aerosol synthesized ones. Attending that catalytic sites are mainly at the edges of a MoS_2 slab, it is common sense to expected that the largest slabs allow a lower promotion and are less active.[16] This effect is clearly the case of the specific hydrogenation activity of *SiCoMoAero 10%* material which is 68% better than that of *SiCoMoImp 10%* catalyst (61% better in the case of *SiCoMoAeros 20%* versus *SiCoMoImp 20%*),

Table 2. Elemental analysis and XPS data of sulfided materials and average MoS_2 slab length.

Materials	MoS_2 [mol%][a)]	Co-MoS_2 [mol%][b)]	Co-S [at%][b)]	MoS_2 slab length [nm][c)]	MoS_2 slab stack number[c)]	MoO_3 before sulfidation [wt%]
SiMoImp 10%	67	-	-	10.1	-	
SiCoMoImp 10%	61	28	41	10.4	5.5	7.8
SiCoMoImp 20%	79	16	36	10.7	6.1	16.4
SiMoAero 10%	71	-	-	4.2	2.7	10.5
SiCoMoAero 10%	79	44	29	5.0	5.2	10.6
SiCoMoAero 20%	75	50	21	4.9	3.7	21.2
Indus. Ref.	80	47	27	3.5	2	21

Obtained from: [a)]the decomposition of Mo(3d) photopeak; [b)]the decomposition of CO(2p) photopeak; [c)]the measure on TEM pictures.

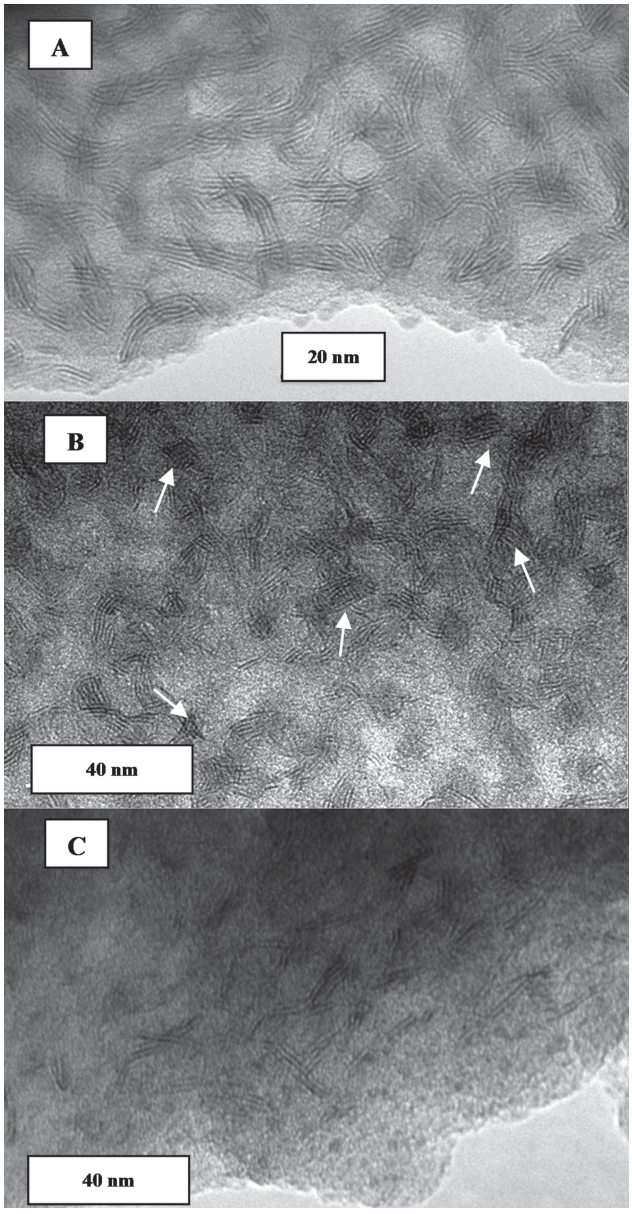

Figure 4. TEM pictures of sufided materials A) SiCoMoImp 10% B) SiCoMo Aero 10% C)SiMo Aero 10%. White arrows point out supposed entangled labs.

due to mean slab length twice smaller (10 and 5 nm respectively for impregnated and one-pot sprayed catalysts). However, slabs obtained by spray drying (SiCoMoAero 10 and 20% catalysts) present higher specific activity, reduced specific activity and TOF than the industrial catalyst (Table 3), which is more surprising attending that industrial catalyst mean slab size is 3.5 nm (see supporting information for industrial catalyst TEM pictures), and present very similar sulfidation and cobalt promotion rates. How to explain then the high promotion rate of the large slabs observed on *SiCoMoAero* catalysts?

This puzzling and reproducible enhancement of hydrogenation activity of slabs issued from sulfidation of directly sprayed

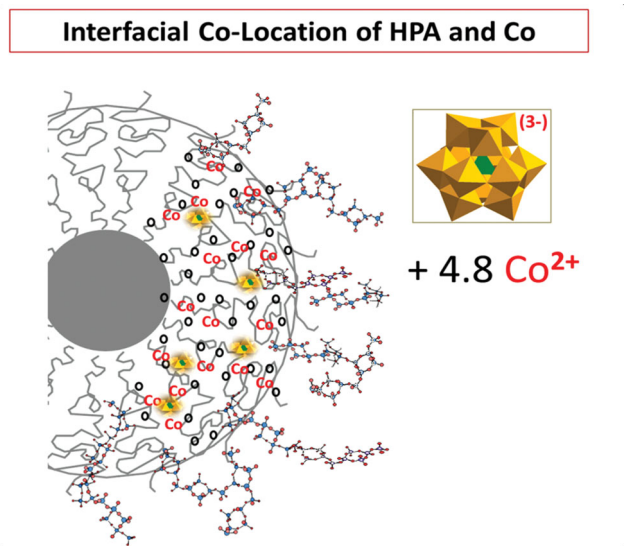

Figure 5. Scheme of the colocation of Co(II) cation and HPA anion. During the solution drying, positive charges of cobalt centres complexed by PEO drive the HPA within the micelle corona.

Table 3. Catalytic characterizations in toluene hydrogenation.

Materials	Specific Activity[a)]	Reduced Specific Activity[b)]	Activity [mmol g^{-1} h^{-1}]	TOF[c)]
SiCoMoImp 10%	0.70	1.15	0.49	6.98
SiCoMoImp 20%	0.58	0.73	0.81	10.07
SiMoAero 10%	0.10	0.14	0.07	-
SiCoMoAero 10%	1.18	1.49	0.82	7.44
SiCoMoAero 20%	0.95	1.27	1.32	5.28
Indus. Ref.	0.78	0.98	1.14	4.15

Obtained from: [a)]given in mol of toluene per mol of molybdenum and per hour; [b)]given in mol of toluene per mol of sulfided Mo and per hour; [c)]given in mol of toluene per mol of cobalt promoted into MoS_2 sheets and per hour.

catalysts may be due to several phenomena. The first reflex of the catalysis scientist is to consider a possible better compromise in between MoS_2 slabs length and stacking favouring hydrogenation. Yet, no evident correlation could be found in between slabs structural parameters and slab hydrogenation activities. Another more unusual possibility lies in the unusual entangled and curved geometry of the slabs produced into our catalysts. Two possible classes of effects can possibly produce such an effect.

(i) A possible anisotropy of MoS_2 slabs (already mentioned in the reference 16). Indeed, the mean slab size is only observed by TEM along the sulfur plans and we cannot determine their dimensions in 3D. If one does not consider possible confining effects onto the hydrogenation reaction itself, a higher catalytic activity could be due to the fact that MoS_2 crystallites have to grow within an interconnected network of mesopores. An anisotropic morphology of the slabs increasing the number of edge sites compare to an isotropic slab, it is likely to explain for a higher hydrogenation activity. So far, we have no experimental evidence in this direction.

(ii) The vermicular structure of pore network contains numerous interconnections in which different growing MoS_2 crystallites seems to compete for space and create entangled slabs as it can be observed in TEM picture (arrows, Figure 4 and SI-5). The small van de Waals cohesion energy of a MoS_2 sheet with its mother slab is very likely to promote the easy formation such entangled domains. In there, twisting and or curved sheets could promote defects as in the case of curved nanostructure. Such curvature effect was recently shown able to create additional sites for metal promotion at the surface of MoS_2 sheets, leading to higher activity than expected from slab length and stack number.[17] Defects being the quality of catalysts, these structural differences are likely to promote the better catalytic activity reproducibly observed for our aerosol processed catalysts. A detailed analysis of such hypothesis will only be made possible by the development of a reliable method allowing the determination of the number and the amplitude of the curvatures of MoS_2 slabs. Such a tool, does not exist yet.

(iii) Finally, the formation of curved MoS_2 sheets may distort the geometry of reactive sites at the edge of MoS_2 sheets. If such a distortion is confirmed, it is very likely to promote a decrease of the cohesion energy of the active site at the edge of the slabs, known to be directly correlated with the catalytic activity of such a catalyst. Literature data proves indeed that this mean cohesion energy is 33 kCal/mol for MoS_2, while an optimum of 32 kCal/mol is wished.[24] A decrease of 4% of this energy is likely to be provided by curved MoS_2 sheets such as that observed in our material. Yet, a dedicated study is required for addressing properly the amplitude of this effect and quantifying unambiguously the degree of curvature of MoS_2 sheets in our materials. Some DFT modelization is required to explore the exact catalytic potential of such deformations.

In spite of the limited comprehension that we have at the moment of the better catalytic properties of directly sprayed $CoMo/SiO_2$, this first series of catalytic test successfully demonstrated the interest that exists in the development of synthetic pathways for the direct synthesis of homogeneously loaded metal-sulfides catalysts. A more detailed investigation of the catalytic properties of those materials is performed at the moment for evaluating in depth recycling and HDS catalytic properties and gaining a better understanding of the advantages and the limits of our synthetic approach.

3. Conclusion

The first one-pot synthesis of mesoporous $CoMo/SiO_2$ composite via aerosol route is reported in this paper. A precise control of textural and structural properties of the spray-dried materials was obtained by an appropriate gestion of the physico-chemical system during solution droplet evaporation (electrostatic and complexation interactions between cobalt-molybdenum precursors and surfactant species), allowing for the precise localization of the oxometallic phase at the hybrid surfactant/silica interface. The sulfidation of these materials lead to different MoS_2 slab morphology regarding to the localization of the oxometallic phase in the wall or in the pore of the silica matrix. Entangled Co-MoS_2 slabs located in the pore of the matrix exhibit better specific catalytic performance in toluene hydrogenation than the equivalent commercial catalysts with similar MoS_2 loading and optimized Co/MoS_2 ratio.

Because such procedure demonstrates outstanding features of one-pot synthesis of large structured pores $CoMo/SiO_2$ composite presenting high hydrogenating activity and the spray drying route is known to be versatile[18] and easily up-scalable to industrial production the present work has been extensively patented.[19–23]

4. Experimental Section

Chemicals: Tetraethyl orthosilicate (TEOS), hydrochloric acid (HCl, 37 wt%), poly(ethylene glycol)-*block*-poly(propylene glycol)-*block*-poly(ethylene glycol) (Pluronic P123, $[EO]_{106}$-$[PO]_{70}$-$[EO]_{106}$, Mn ~5,800 g/mol), phosphomolybdic acid ($H_3PMo_{12}O_{40},xH_2O$), cobalt hydroxide ($Co(OH)_2$) and absolut etanol (EtOH) have been purchased from sigma-aldirch and used without further purification.

Catalyst Preparation: A) tetraethyl orthosilicate (7.5 g) was hydrolyzed under stirring overnight in an aqueous solution (12.1 g, pH 2, HCl 0.02 M). The desired amount of $H_3PMo_{12}O_{40}$ (10 wt% of MoO_3 in the calcined material) and $Co(OH)_2$ (Co/Mo = 0.36 mol) was dissolved in distilled water (pH 2, HCl 0.02 M) and was added at the end of this hydrolysis step. Solution B) block-copolymer Pluronic P123 $[EO]_{106}$-$[PO]_{70}$-$[EO]_{106}$ (2.2 g) was dissolved in ethanol (5.3 g) and water (22.5 g, pH 2, HCl 0.02 M) and left under magnetic stirring for one night. Solutions A and B are then put together (molar composition of the final solution TEOS:$H_3PMo_{12}O_{40}$:$Co(OH)_2$:H_2O:HCl:EtOH:P123; $0.93{:}0.37{*}10^{-2}{:}0.18{*}10^{-1}{:}50{:}0.9{*}10^{-2}{:}3{:}0.01$) and sprayed with a B-290 atomizer from Büchi with these parameters: input temperature: 220 °C, atomization gaz flow: 600 L/h, succion flow: 35 m^3/h, pump flow: 9 cm^3/min. The recovered powder was then calcined under static air at 130 °C for 2h (2°/min) and then 350 °C for 12 h (2°/min). Some 20 wt% catalysts have also been prepared in a similar way.

Characterization of Textural and Structural Properties: N_2 physisorption measurements were made on a ASAP Micromeritics 2000 apparatus. SSA was determined by the BET method in the 0.05-0.30 p/p0 range. Pore volume is determined by the amount of N_2 adsorbed at p/p_0 = 98. Wide-angle X-ray diffraction measurements were realized with a Bruker d8 facility. SAXS was performed on a Rigaku SMAX3000. High-resolution transmission electron microscopy (TEM) was carried out with a Tecnai Twin Spirit G2 (120 kV). Scanning electron microscopy (SEM) was carried out with a Hitachi S-3400N device, EDX cartographies were recorded with a Oxford Instrument X-max detector.

Catalytic Test: Toluene hydrogenation test was conducted in fluidized bed reactor at 623 K and 6 MPa. The liquid feed contained 74.1 wt% cyclohexane (used as solvent), 20.0 wt% toluene, 5.9 wt% dimethyldisulfide, used as sulfiding agent. H_2 /feed ratio was constant and equal to 450 Nl/L. The liquid feed flow was 16 cm^3/h (LHSV = 4 h^{-1}) during the sulfidation stage and 8 cm^3/h (LHSV = 2 h^{-1}) during the catalytic test. Catalysts were pelletized, crushed and sieved in the 150 – 500 µm range. This fraction was diluted in solid SiC (4 cm^3 for 4 cm^3 of catalyst). After sulfidation (2 °C/min followed by 2 h at 350 C), conversions were determined by the analysis of effluent through on-line gas chromatography every 45 min after the first measurement. Catalytic results were expressed in terms of toluene hydrogenation specific activity calculated from toluene conversion (after equilibration time of 5 hours), amount of Mo and Co and time on stream. The reference is an industrial catalyst made by wetness incipient impregnation of a large surface γ-alumina. It is loaded at 21 wt% of MoO_3 before sulfidation with an optimal Co/Mo.

Supporting Information

Supporting Information is available from the Wiley Online Library or from the author.

Acknowledgements

F.C.J kindly thanks N.Lett, J. Marin and S. Rafik-Clément for their technical support, M. Girleanu and A.-S Gay for HAADF STEM images, and Ovidiu Ersen from IPCMS of Strasbourg for TEM images.

Received: June 25, 2013
Published online: August 28, 2013

[1] J. Grimblot, *Catal. Today.* **1998**, *41*, 111–128.
[2] E. Etienne, E. Ponthieu, E. Payen, J. Grimblot, *J. Non-Cryst. Solids* **1992**, *147*, 764–768.
[3] L. Lebihan, C. Mauchausse, L. Duhamel, J. Grimblot, E. Payen, *J. Sol-Gel Sci. Technol.* **1994**, *2*, 837–842.
[4] R. Van Veen, P. A. J. Hendriks, R. Andrea, E. J. G. Romers, A. E. Wilson, *J. Phys. Chem.* **1990**, *94*, 5282–5285.
[5] A. Griboval, P. Blanchard, E. Payen, M. Fournier, J. L. Dubois, *Catal. Today.* **1998**, *45*, 277–283.
[6] T. Yanagisawa, T. Shimizu, K. Kuroda, C. Kato, *Bull. Chem. Soc. Jpn.* **1990**, *63*, 988–992.
[7] J. S. Beck, J. C. Vartuli, W. J. Roth, M. E. Leonowicz, C. T. Kresge, K. D. Schmitt, C. T. W. Chu, D. H. Olson, E. W. Sheppard, *J. Am. Chem. Soc.* **1992**, *114*, 10834–10843.
[8] Q. Huo, D. Margolese, U. Ciesla, P. Feng, T. Gier, P. Sieger, R. Leon, P. Petroff, F. Schüth, G. Stucky, *Nature* **1994**, *368*, 317–321.
[9] V. Dufaud, F. Lefebvre, *Materials* **2010**, *3*, 682–703.
[10] V. Dufaud, F. Lefebvre, G. P. Niccolai, M. Aouine, *J. Mater. Chem.* **2009**, *19*, 1142.
[11] a) C. J. Brinker, Y. Lu, A. Sellinger, H. Fan, *Adv. Mater.* **1999**, *11*, 579–585; b) M. Santiago, A. Restuccia, F. Gramm, J. Pérez-Ramírez, *Micro. Meso. Mater.* **2011**, *146*, 76–81.
[12] S. Pega, C. Boissière, D. Grosso, T. Azais, A. Chaumonnot, C. Sanchez, *Angew. Chem. Int. Ed.* **2009**, *48*, 2784–2787.
[13] D. P. Debecker, M. Stoyanova, F. Colbeau-Justin, U. Rodemerck, C. Boissière, E. Gaigneaux, C. Sanchez, *Angew. Chem. Int. Ed.* **2012**, *51*, 2129–2131.
[14] C. Wivel, R. Candia, B. S. Clausen, S. Mørup, H. Topsøe, *J. Catal.* **1981**, *68*, 453–463.
[15] C. Boissière, M. U. Martines, A. Larbot, E. Prouzet, *J. Membrane Sci.* **2005**, *257*, 17.
[16] S. Kasztelan, H. Toulhoat, J. Grimblot, J. P. Bonnelle, *Appl. Catal.* **1984**, *13*, 127–159.
[17] A. Nogueira, R. Znaiguia, D. Uzio, P. Afanasiev, G. Berhault, *Appl. Catal. A* **2012**, *429–430*, 92–105.
[18] C. Boissière, D. Grosso, A. Chaumonnot, L. Nicole, C. Sanchez, *Adv. Mater.* **2011**, *23*, 599–623.
[19] A. Chaumonnot, C. Sanchez, C. Boissière, F. Colbeau-Justin, A. Bonduelle, WO/2012/085358, **2012**.
[20] A. Chaumonnot, C. Sanchez, C. Boissière, F. Colbeau-Justin, A. Bonduelle WO/2012/085356, **2012**.
[21] A. Chaumonnot, C. Sanchez, C. Boissière, F. Colbeau-Justin, K. Marchand, E. Devers, A. Bonduelle, D. Uzio, A. Daudin, B. Guichard, Uzio, WO2012085355A1, **2012**.
[22] A. Chaumonnot, C. Sanchez, C. Boissière, F. Colbeau-Justin, A. Bonduelle, WO/2012/085354, **2012**.
[23] D. P. Debecker, F. Colbeau-Justin, C. Sanchez, A. Chaumonnot, M. Berthod, WO/2013/011209, **2013**.
[24] H. Toulhoat, P. Raybaud, *Catalysis by Transition Metal Sulphide, from Molecular Theory to Industrial Application*, Technip, Paris **2013**.